

Article

Effects of Reinforcing Fiber Strength on Mechanical Properties of High-Strength Concrete

Hyun-Do Yun ¹, Seong-Hoon Lim ¹ and Won-Chang Choi ^{2,*}

¹ Department of Architectural Engineering, Chungnam National University, Daejeon 305-764, Korea; wiseroad@cnu.ac.kr (H.-D.Y.); sunghun0505@naver.com (S.-H.L.)

² Department of Architectural Engineering, Gachon University, Gyeonggi-do 461-701, Korea

* Correspondence: wchoi@gachon.ac.kr; Tel.: +82-31-750-5335

Received: 30 August 2019; Accepted: 2 October 2019; Published: 21 October 2019



Abstract: This paper investigates the effects of the tensile strength of steel fiber on the mechanical properties of steel fiber-reinforced high-strength concrete. Two levels of steel fiber tensile strength (1100 MPa and 1600 MPa) and two steel fiber contents (0.38% and 0.75%) were used to test the compression, flexure, and direct shear performance of steel fiber-reinforced high-strength concrete specimens. The aspect ratio for the steel fiber was fixed at 80 and the design compressive strength of neat concrete was set at 70 MPa to match that of high-strength concrete. The performance of the steel fiber-reinforced concrete that contained high-strength steel fiber was superior to that which contained normal-strength steel fiber. In terms of flexural performance in particular, the tensile strength of steel fiber can better indicate performance than the steel fiber mixing ratio. In addition, a compression prediction model is proposed to evaluate compression toughness, and the model results are compared. The predictive model can anticipate the behavior after the maximum load.

Keywords: steel fiber-reinforced concrete; tensile strength; fiber content; compressive strength; flexure; direct shear

1. Introduction

Steel fiber-reinforced concrete (SFRC), which incorporates steel fiber into the concrete mixture, not only improves the material's shear strength and tensile strength, but also improves its impact resistance, fatigue life, and ductility, and controls crack growth via the crosslinking of the fibers [1]. Research into SFRC has been actively conducted since the 1970s, with studies investigating various mix ratios of steel fiber with respect to the steel fiber's aspect ratio and tensile strength [2,3]. Among the various parameters that influence the performance of SFRC, the mix ratio and aspect ratio of the steel fiber are the most prominent [4]. Köksall et al., 2012 studied the mechanical properties of SFRC with variables of concrete compressive strength and tensile strength of steel fiber. They concluded that variations of the mechanical properties of SFRC were insignificant when using normal concrete. Depending on the compressive concrete strength, the mechanical properties were highly affected in SFRC. In practice, when an amount of steel fibers are mixed in excess, the fibers reduce the mixture's workability during the pouring operation and diminish the positive effects of incorporating the fibers [5]. With advancements in manufacturing, various types and tensile strengths of steel fiber are available commercially, and high-strength steel fiber has been shown to improve the mechanical performance of SFRC [6].

This study was focused primarily on the effects of the tensile strength (rather than the aspect ratio) of steel fiber on the mechanical properties of SFRC. The tests performed were compression, flexure, and direct shear tests of SFRC specimens.

2. Experimental Program

2.1. Materials and Fabrication

High-strength concrete with the design compressive strength concrete of 70 MPa was used in this study. Table 1 presents the mix proportions for concrete used in the study.

Table 1. Mix proportions for concrete.

W/B (%)	Air (%)	S/a (%)	Unit Weight (kg/m ³)				
			Water	Cement	Silica fume	Sand	Gravel
33	4	45	157	451	24	717	860

W/B: water-to-binder ratio, S/a: sand-to-aggregate ratio.

The two main variables used for the three types of tests were fiber content and fiber tensile strength. The two steel fiber contents used in this study were 0.38% and 0.75 percent. According to American Concrete Institute (ACI) 318-14 (2014) [7], the fiber content of 0.75% for SFRC is based on the minimum amount of fiber content for substitution of the minimum shear reinforcement. The tensile strength values of the steel fiber used in this study were 1100 MPa and 1600 MPa. The end-hooked steel fiber was 0.75 mm in diameter and 60 mm in length. Figure 1 shows the dimensions and various configurations of the steel fibers used in the SFRC. The fiber aspect ratio of 80 was selected and fixed for this study. Related research results regarding the performance of SFRC with various aspect ratios of steel fiber can be found elsewhere [8,9].

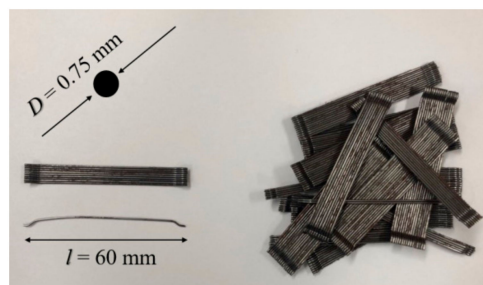


Figure 1. Dimensions and configurations of steel fiber used in this study.

The cylindrical and prismatic specimens that were fabricated for the tests to determine the mechanical properties were cured for 24 h in a mold after casting and water-cured at 20 °C ± 1 °C for 29 days.

2.2. Test Set-Ups

For the compression tests, three cylindrical specimens 150 mm in diameter and 300 mm in height were fabricated for each mix design according to KS F2403 (2014) [10]. Transverse reinforcement was placed in a compression mold to improve the confining force of the compression member so that the post behavior could be monitored after the maximum load was applied. Figure 2 shows details regarding the transverse reinforcement in the compression specimen.

The compression tests were conducted using a 2000-kN universal testing machine (UTM). Figure 3a shows the compression test set-up. Linear variable differential transducers (LVDTs) were installed to measure the deformation of the compression specimens. According to KS F2405, in order to determine the compressive strength of concrete, loading is applied with a force control of 0.6 MPa/s ± 0.4 MPa/second. However, in this study, compression loading was applied with a displacement rate of 0.1 mm/min to observe the post peak behavior.

The flexural tests were conducted in accordance with ASTM C 1609 [11]. Three prismatic specimens with dimensions of 150 mm × 150 mm × 550 mm were fabricated using each mixture. Three-point

loading was applied using a 200-kN UTM with a displacement rate of 0.3 mm/minute. Figure 3b shows the flexural test set-up and the LVDTs that were installed to measure the displacement at the center of the specimen.

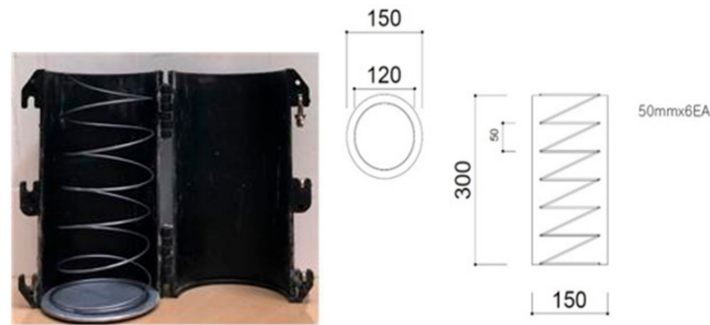


Figure 2. Reinforcement details for compression specimen.

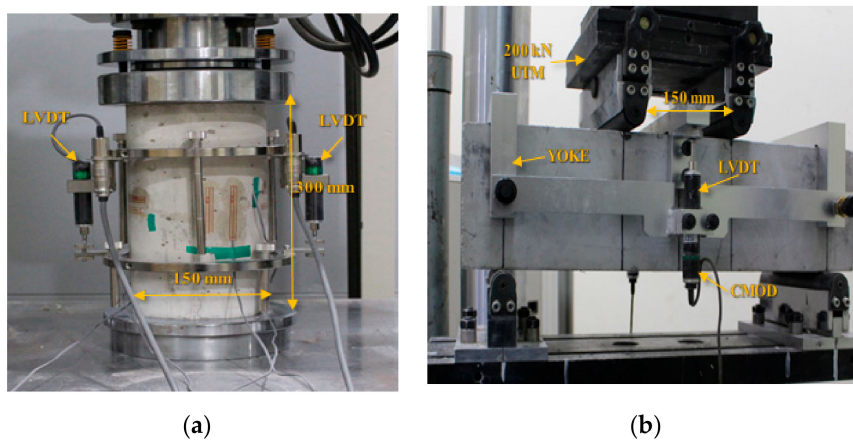


Figure 3. Test set-ups for (a) compression and (b) flexural tests.

The direct shear tests were conducted in accordance with JSCE-SF6 (1990) [12]. Three rectangular specimens, each 150 mm × 150 mm × 550 mm, were fabricated to evaluate shear behavior. Loading was applied using a 2000-kN UTM with a displacement rate of 0.1 mm/minute. Figure 4 shows the direct shear test set-up and the four LVDTs that were installed to measure the horizontal and vertical displacements of the specimens. The specimens were sawn to create a 5-mm wide, 15-mm deep notch on the bottom of each specimen to induce direct shear failure.

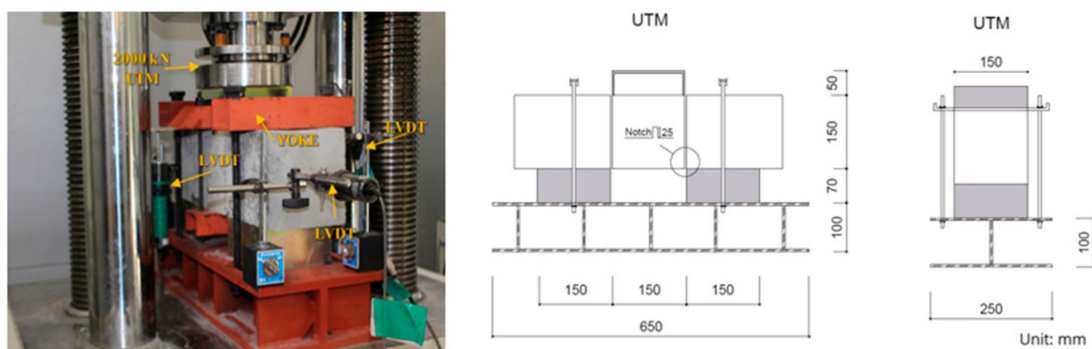


Figure 4. Direct shear test set-up and installed instruments.

3. Results and Discussion

3.1. Compressive Behavior of SFRC with High-Strength Steel Fiber

Table 2 presents the compressive test results that include the compressive strength, elastic modulus, and ultimate compressive strain values, and the Poisson's ratios. The table lists the averaged values obtained from the three specimens for each mixture. The mixture specimen designations used for the compressive tests reflect the tensile strength of the steel fiber, the steel fiber content (its volume fraction), and the presence of transverse reinforcement. For example, HS-0.75-S indicates that the specimen has a high tensile strength (HS) (1600 MPa), 0.75% fiber, and transverse reinforcement (S); NS indicates normal strength; CON indicates the control concrete mixture, and N indicates no transverse reinforcement.

Table 2. Compressive behavior of steel fiber-reinforced concrete (SFRC).

Mixture	f'_c (MPa)	Elastic Modulus (GPa)	ϵ_c ($\mu\epsilon$)	Poisson's Ratio
CON-N	60.6 (± 1.4)	32.0 (± 0.8)	2350 (± 70)	0.21 (± 0.01)
NS-0.75-N	62.8 (± 6.0)	32.4 (± 2.8)	2591 (± 566)	0.22 (± 0.01)
HS-0.38-N	67.5 (± 1.6)	35.0 (± 0.8)	2378 (± 49)	0.21 (± 0.02)
HS-0.75-N	67.04 (± 0.2)	31.3 (± 2.9)	2978 (± 17)	0.23 (± 0.01)
CON-S	62.0 (± 1.9)	32.0 (± 0.0)	2449 (± 10)	0.22 (± 0.02)
NS-0.75-S	65.6 (± 0.8)	32.4 (± 0.4)	2583 (± 88)	0.21 (± 0.01)
HS-0.38-S	67.5 (± 2.0)	35.9 (± 4.4)	2225 (± 17)	0.23 (± 0.01)
HS-0.75-S	68.4 (± 1.2)	32.7 (± 1.7)	2772 (± 3)	0.24 (± 0.03)

The compressive strength of the SFRC specimens with 0.75% high-strength steel fiber was improved by about 10% compared to that of the ordinary concrete (CON) specimens without steel fiber. Also, a comparison of the HS-0.75 and NS-0.75 specimens shows that superior results were obtained for the HS-0.75 specimens that contained high-strength steel fiber compared to the specimens that contained normal-strength steel fiber. The compressive strength values of the HS-0.75 and HS-0.38 specimens with different fiber contents are similar because tensile strength is a more dominant parameter than the mixing ratio in compressive strength tests. The compressive strength increased by about 2 MPa–3 MPa when transverse reinforcement was placed, but it showed little or no change in the SFRC specimens with high-strength steel fiber.

Figure 5 shows the vertical and horizontal deformations of the different compression test specimens that were measured by gauges installed in the concrete. The results show that the horizontal strain increased abruptly in the specimens without steel fiber and in the SFRC specimens with normal-strength steel fiber, whereas the SFRC specimens with high-strength steel fiber deformed only slightly in the horizontal direction. The incorporation of steel fiber reinforcement and transverse reinforcing steel in the concrete with low vertical strain and the SFRC specimens had a positive effect in terms of resistance to vertical strain, in particular for the ordinary concrete (CON) specimens and the SFRC specimens with normal-strength steel fiber.

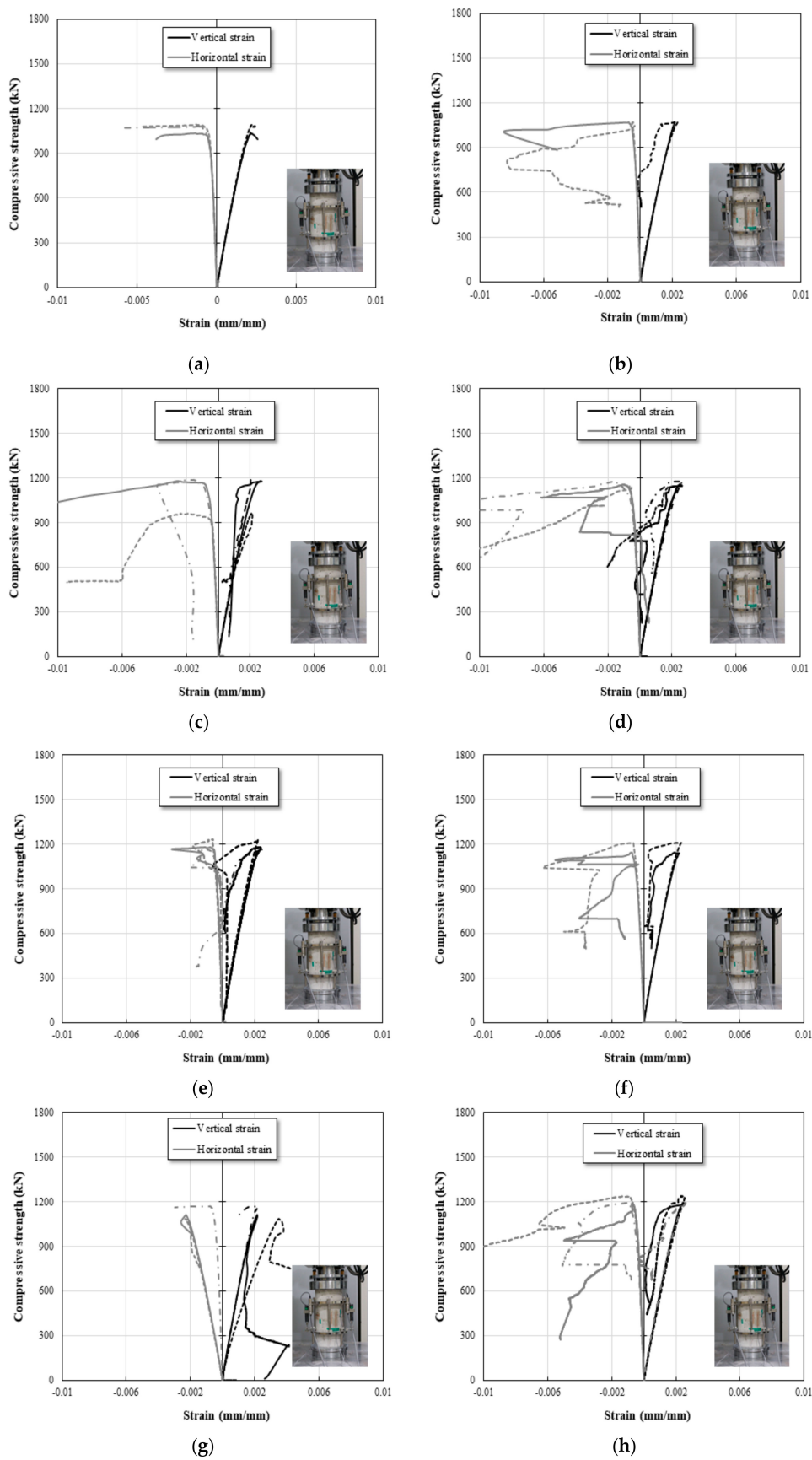


Figure 5. Vertical and horizontal strain values of compression test specimens. (a) CON-N; (b) CON-S; (c) NS-0.75-N; (d) NS-0.75-S; (e) HS-0.38-N; (f) HS-038-S; (g) HS-075-N; (h) HS-0.75-S.

3.2. Flexural Behavior of SFRC Specimens with High-Strength Steel Fiber

Figure 6 shows the relationship between flexural strength and crack open-mouth displacement (COMD) for the SFRC specimens. The results indicate that the HS-0.75 and HS-0.38 specimens with high-strength steel fiber show ductile fracture behavior, whereas the NS-0.75 specimens with normal-strength steel fiber show brittle fracture behavior.

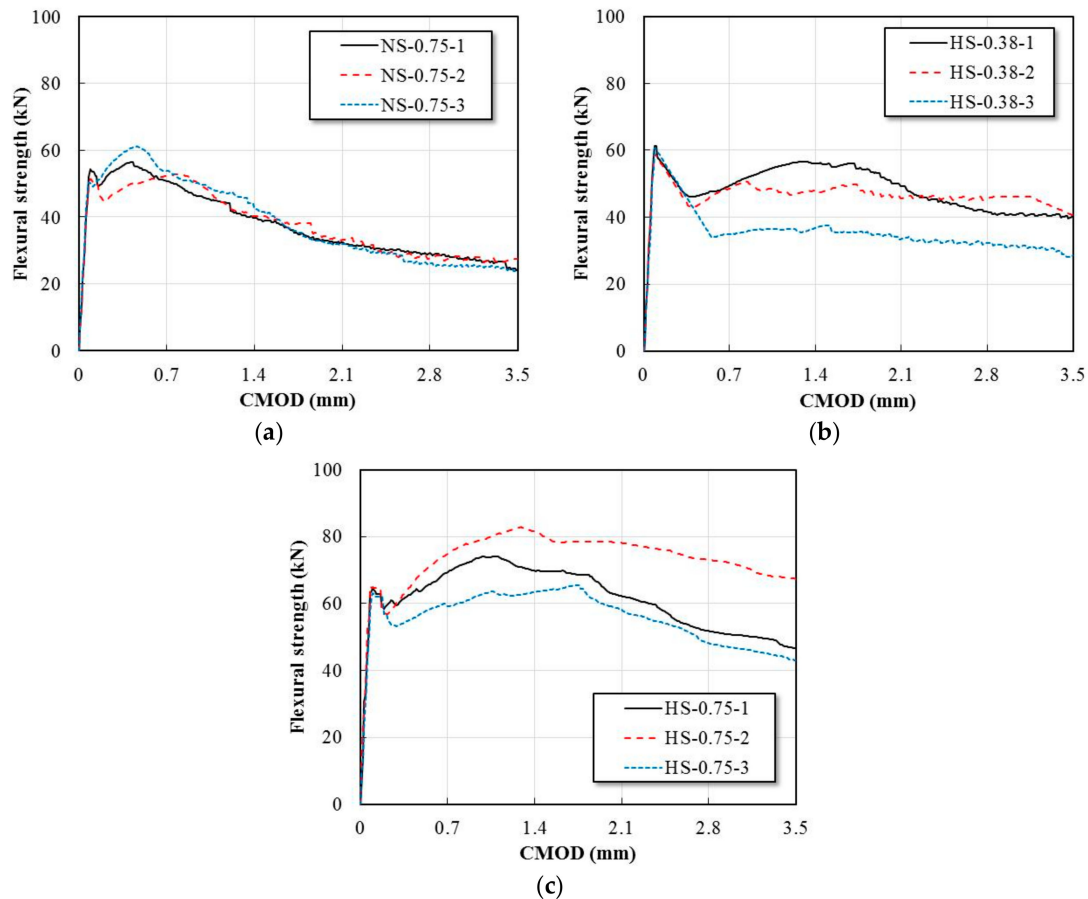


Figure 6. Flexural strength versus crack open-mouth displacement (COMD) curves for SFRC specimens. (a) NS-0.75; (b) HS-0.38; (c) HS-0.75.

The flexural performance was evaluated using a flexural toughness (TF) index. This toughness index was computed at displacements of 1/300 and 1/150 of the span length. Equations (1) and (2) were used to compute the TF values for these two displacements, respectively.

$$TF_{f,300} = \frac{300T_{f,300}}{f_1bh^2} \tag{1}$$

$$TF_{f,150} = \frac{150T_{f,150}}{f_1bh^2} \tag{2}$$

where TF is flexural toughness; $TF_{f,150}$ and $TF_{f,300}$ indicate displacement at 1/150 and 1/300 of the span length, respectively; f_1 is the initial crack strength; b (mm) is width; and h (mm) is the height of the specimen [13].

Table 3 summarizes the initial crack strength, displacement at the initial crack strength, flexural strength, displacement at the flexural strength, flexural toughness, and flexural toughness index values.

Table 3. Flexure test results for flexural performance of SFRC mixtures.

Mixture	f_1 (kN)	δ_1 (mm)	f_p (kN)	δ_p (mm)	$TF_{f1,300}$ (kN·mm)	$TF_{f1,150}$ (kN·mm)	$T_{f1,300}$	$T_{f1,150}$
CON	59.46 (±3.94)	0.08 (±0.0)	59.46 (±3.94)	0.08 (±0.0)	-	-	-	-
NS-0.75	51.21 (±1.59)	0.13 (±0.0)	56.76 (±3.35)	0.20 (±0.16)	71.97 (±2.65)	119.37 (±1.71)	0.94 (±0.06)	0.78 (±0.03)
HS-0.38	58.85 (±1.47)	0.12 (±0.03)	60.47 (±0.96)	0.09 (±0.0)	68.84 (±7.31)	132.66 (±16.80)	0.78 (±0.10)	0.75 (±0.11)
HS-0.75	63.26 (±1.09)	0.15 (±0.02)	74.22 (±7.11)	1.34 (±0.30)	97.91 (±8.10)	194.54 (±20.63)	1.03 (±0.07)	1.02 (±0.09)

The SFRC specimen with 0.75% high-strength steel fiber was found to improve initial cracking resistance, flexural strength, and flexural toughness. The variable, tensile strength of fiber, is more critical in terms of flexural performance than fiber contents. With regard to the effect on fiber content, the initial cracking strength of the HS-0.38 specimen is similar to that of the HS-0.75 specimen, but significant changes were observed in terms flexural strength.

The initial cracking strength of the NS-0.75 specimens was about 10% lower than that of the HS-0.75 specimens. After reaching maximum flexural strength, the NS-0.75 specimens showed a large reduction in load, unlike the specimens reinforced with high-strength steel fiber. The TF values of the SFRC specimens with respect to fiber content increased with an increase in fiber content.

Based on the toughness index, which reflects the tensile strength of steel fiber, the increase in tensile strength shows a slight effect at a span ratio of 1/300, but the flexural toughness index increased significantly at the span ratio of 1/150. These results show that fiber tensile strength is closely related to end behavior in flexural tests. In the case of the SFRC specimens with normal-strength steel fiber, the fiber failed to resist the load when the specimen failed. However, in the case of the SFRC specimens with high-strength steel fiber, the high-strength steel fiber suppressed crack formation throughout the specimen and improved the flexural strength via its close adherence to the concrete, thereby ensuring ductility and preventing breakage. In short, the flexural toughness index values were higher for the SFRC specimens that contained high-strength steel fiber than for the other specimens.

3.3. Direct Shear Behavior of SFRC Specimens

Figure 7 presents the direct shear test results with respect to fiber content in terms of typical load versus deflection. The results indicate that the SFRC specimens with high tensile strength steel fiber have greater shear strength compared to the specimens with normal tensile strength steel fiber. The maximum shear strength values of the HS-0.38 and HS-0.75 specimens are similar. However, the shear toughness of HS-0.75 is more than twice that of HS-0.38, as mentioned in the previous section. Addition of steel fibers in plain concrete specimen improves the shear strength as confirmed in literature [14].

Shear stress can be computed using Equation (3).

$$\tau_{max} = \frac{P_{max}}{2bh} \quad (3)$$

where τ_{max} is the maximum shear stress (MPa); P_{max} is the maximum applied shear load (kN); b (mm) is the width of the specimen, and h (mm) is the height of the specimen.

Figure 8 summarizes the results for the initial shear crack load, maximum shear load, and maximum shear stress. The shear strength of the SFRC specimens with high-strength steel fiber improved by about 20% compared to the CON specimens with ordinary concrete. However, the shear strength of the SFRC specimens with normal-strength steel fiber improved by only about 10 percent.

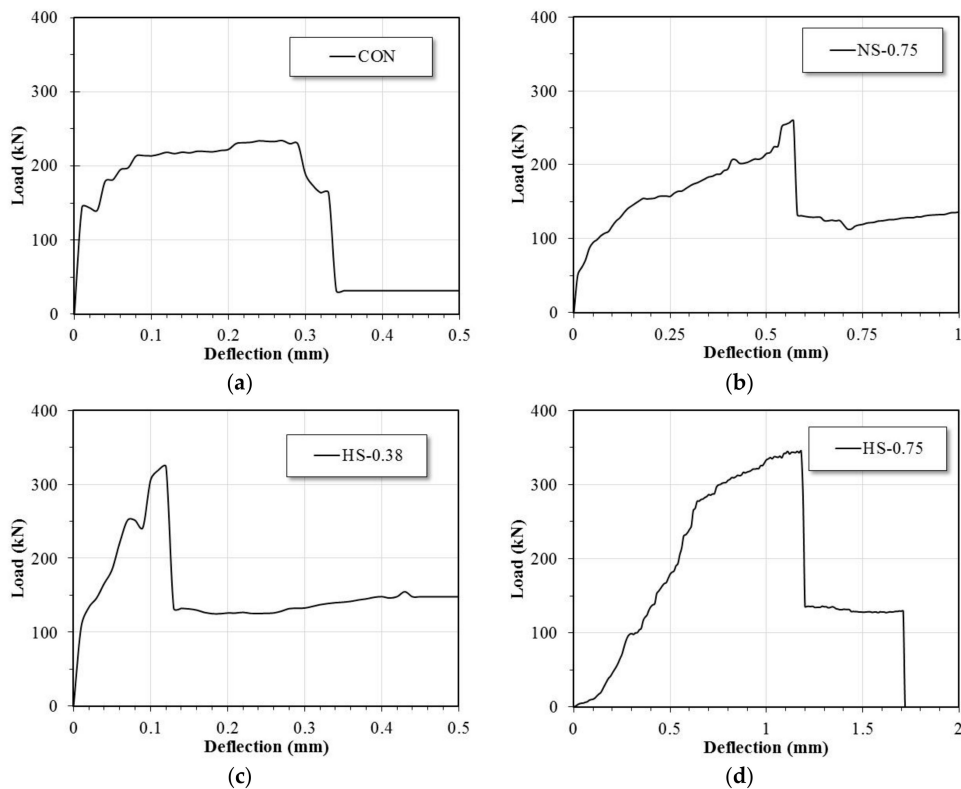


Figure 7. Typical load-deflection curves obtained from direct shear tests. (a) Concrete; (b) NS-0.75; (c) HS-0.38; (d) HS-0.75.

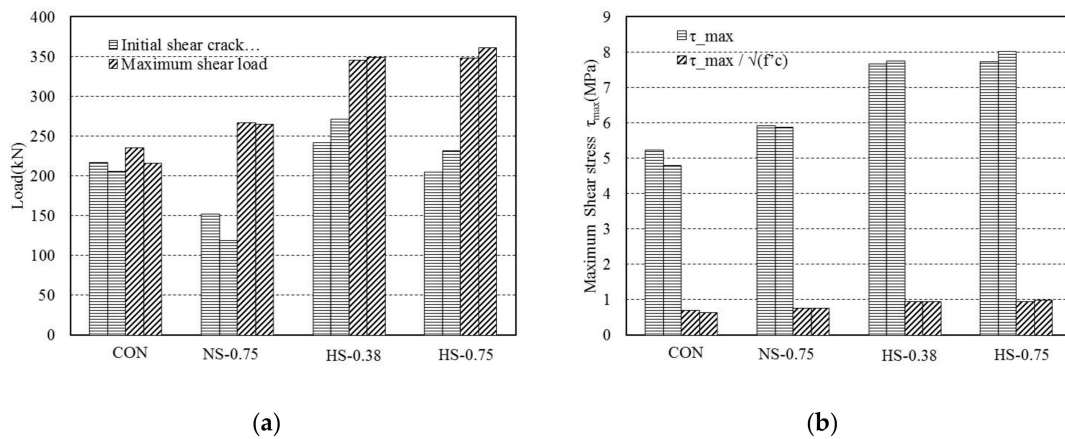


Figure 8. Shear strength of fiber-reinforced concrete. (a) shear load; (b) shear stress.

3.4. Modeling the Compressive Behavior of SFRC

A stress-strain curve for SFRC with end-hooked steel fiber is proposed herein. The compressive behavior of SFRC members can be predicted using Equations (4) through (7), as derived by [15].

$$\frac{f_c}{f'_c} = \frac{A(\epsilon_c/\epsilon_0)}{A - 1 + (\epsilon_c/\epsilon_0)^B} \tag{4}$$

$$A = B = \frac{1}{1 - \frac{f'_c}{\epsilon_c E_c}}, \quad \epsilon_c/\epsilon_0 \leq 1.0 \tag{5}$$

$$A = 1 + 0.723 \left(V_f \frac{l_f}{d_f} \right)^{-0.957}, \quad \varepsilon_c / \varepsilon_0 > 1.0 \quad (6)$$

$$B = \left(\frac{f'_c}{50} \right)^{0.064} \left[1 + 0.882 \left(V_f \frac{l_f}{d_f} \right)^{-0.882} \right], \quad \varepsilon_c / \varepsilon_0 > 1.0 \quad (7)$$

where A and B are coefficients; V_f (%) is fiber content; ε_0 is ultimate strain; E_c is the elastic modulus of concrete; and l_f and d_f are the length and diameter of the fiber, respectively.

Figure 9 presents a comparison between typical, actual behavior under compression and the predictive model results obtained using the proposed Equations (4)–(7). For the specimens with 0.75% steel fiber, the load is shown to decrease sharply or become unstable after reaching the maximum load. The predictive model can anticipate the behavior after the maximum load, and thus, a toughness ratio can be obtained. Similar results can be obtained by using the predictive model Equations (4)–(7) after the maximum load, as shown in Figure 8. The compressive toughness values obtained from the predictive model are closely related to the steel fiber content. Increasing the steel fiber mixing ratio and increasing the tensile strength of the steel fiber are shown to improve the compressive toughness [16]. The compressive toughness also was improved by increasing the mix ratio rather than by increasing the tensile strength.

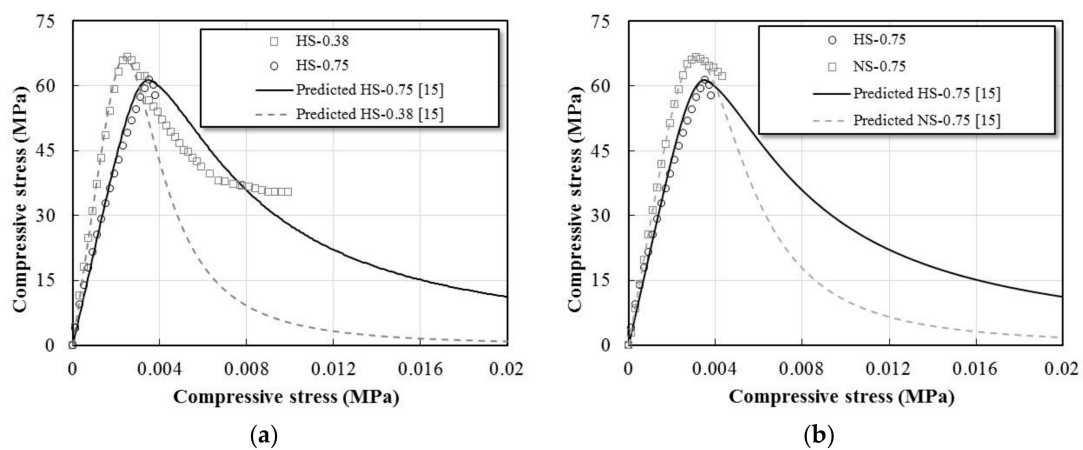


Figure 9. Stress-strain curves of SFRC under compression. (a) With regard to fiber content; (b) With regard to fiber tensile strength.

4. Conclusions

The effects on the mechanical properties of high-strength SFRC with respect to the tensile strength of embedded steel fibers were evaluated in this study using compression, flexure, and direct shear tests. The limited test results led to the following findings.

- (1) With regard to fiber tensile strength, the results show that the compressive strength values are high for the SFRC specimens that contained high-strength steel fiber. When the mix ratio was used as a variable, similar compressive strength values were found at 0.38% and 0.75% steel fiber contents.
- (2) With regard to flexural behavior, the SFRC specimens that contained 0.38% and 0.75% high-strength steel fiber showed similar ductile flexural behavior after initial cracking. However, in terms of flexural strength, the test specimens that contained 0.75% high-strength steel fiber showed superior performance, with more than 30% improvement. In addition, the flexural strength and behavior after initial cracking were excellent for the SFRC specimens that contained 0.75% high-strength steel fiber and were better than the SFRC specimens that contained 0.75% normal strength steel fiber.

- (3) All the SFRC specimens that contained steel fiber showed sufficient shear strength; however, the HS-0.75 specimens exhibited the greatest shear strength and most ductile behavior of all the specimens tested.

Author Contributions: H.-D.Y. contributed to the project idea development and experimental design, and S.-H.L. performed the data analysis and wrote a draft manuscript. W.C. reviewed the final manuscript and contributed to the results discussion and conclusions.

Funding: This work was supported by the Gachon University research fund of 2019 (GCU-2019-0312).

Conflicts of Interest: The authors declare no conflicts of interests regarding the publication of this article.

References

1. Yazıcı, Ş.; Inan, G.; Tabak, V. Effect of aspect ratio and volume fraction of steel fiber on the mechanical properties of SFRC. *Constr. Build. Mater.* **2007**, *21*, 1250–1253. [[CrossRef](#)]
2. Choi, W.C.; Jung, K.Y.; Jang, S.K.; Yun, H.D. The Influence of Steel Fiber Tensile Strengths and Aspect Ratios on the Fracture Properties of High-Strength Concrete. *Materials* **2019**, *12*, 2105. [[CrossRef](#)] [[PubMed](#)]
3. Köksal, F.; Sahin, Y.; Sahin, M. Effect of Steel Fiber Tensile Strength on Mechanical Properties of Steel Fiber Reinforced Concretes. *Spec. Publ.* **2012**, *289*, 129–143.
4. Jeong, G.Y.; Jang, S.J.; Kim, Y.C.; Yun, H.D. Effects of Steel Fiber Strength and Aspect Ratio on Mechanical Properties of High-Strength Concrete. *J. Korea Concr. Inst.* **2018**, *30*, 197–205. (In Korean) [[CrossRef](#)]
5. Koh, K.T.; Kang, S.T.; Park, J.J.; Ryu, G.S. A Study on the Improvement of Workability of High Strength Steel Fiber Reinforced Cementitious Composites. *J. Korea Inst. Struct. Maint. Insp.* **2004**, *8*, 141–148. (In Korean)
6. Song, P.S.; Hwang, S. Mechanical properties of high-strength steel fiber-reinforced concrete. *Constr. Build. Mater.* **2004**, *18*, 669–673. [[CrossRef](#)]
7. ACI Committee 318. *Building Code Requirements for Structural Concrete (ACI 318-14) and Commentary*; American Concrete Institute: Farmington Hills, MI, USA, 2014.
8. Jang, S.J.; Ahn, K.L.; Yun, H.D. Effects of Aggregate Size and Fiber Volume Fraction on Flexural Properties of Steel Fiber Reinforced Concrete (SFRC). *J. Archit. Inst. Korea* **2015**, *312*, 45–54. (In Korea, with English abstract).
9. Jang, S.J.; Jeong, G.Y.; Yun, H.D. Use of steel fibers as transverse reinforcement in diagonally reinforced coupling beams with normal and high-strength concrete. *Constr. Build. Mater.* **2018**, *187*, 1020–1030. [[CrossRef](#)]
10. Korean Standards Association. *Standard Test Method of Making and Curing Concrete Specimens*; Korean Standards Association: Seoul, Korea, 2014. (In Korean)
11. American Society for Testing and Materials. *Standard Test Method for Flexural Performance of Fiber-Reinforced Concrete (Using Beam with Third-Point Loading)*; American Society for Testing and Materials: West Conshohocken, PA, USA, 2012.
12. Japan Society of Civil Engineer. *Method of Test for Shear Strength Fiber Reinforced Concrete*; Japan Society of Civil Engineer: Tokyo, Japan, 1990; Available online: http://library.jsce.or.jp/Image_DB/spec/con_lib/no03/CLIno03_0067.pdf (accessed on 26 August 2019).
13. Jang, S.J.; Yun, H.D. Combined effects of steel fiber and coarse aggregate size on the compressive and flexural toughness of high-strength concrete. *Compos. Struct.* **2018**, *185*, 203–211. [[CrossRef](#)]
14. Rao, G.A.; Rao, A.S. Toughness indices of steel fiber reinforced concrete under mode II loading. *Mater. Struct.* **2009**, *42*, 1173.
15. Lee, S.C.; Oh, J.H.; Cho, J.Y. Compressive behavior of fiber-reinforced concrete with end-hooked steel fibers. *Materials* **2015**, *8*, 1442–1458. [[CrossRef](#)] [[PubMed](#)]
16. Mostafazadeh, M.; Abolmaali, A. Shear behavior of synthetic fiber reinforced concrete. *Adv. Civ. Eng. Mater.* **2016**, *5*, 371–386. [[CrossRef](#)]

